ARTICLE IN PRESS

Atmospheric Pollution Research xxx (xxxx) xxx–xxx

HOSTED BY

ELSEVIER

Contents lists available at ScienceDirect

Atmospheric Pollution Research

journal homepage: www.elsevier.com/locate/apr

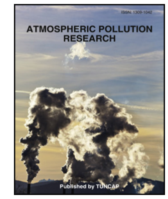

The role of environmental factors in ozone uptake of *Pinus mugo* Turra

Svetlana Bičárová[a,*], Zuzana Sitková[b], Hana Pavlendová[b], Peter Fleischer Jr.[c,d], Peter Fleischer Sr.[c,e], Andrzej Bytnerowicz[f]

[a] *Institute of Earth Science of the Slovak Academy of Sciences, Stará Lesná, 059 60 Tatranská Lomnica, Slovakia*
[b] *National Forest Centre–Forest Research Institute Zvolen, T. G. Masaryka 22, 960 92 Zvolen, Slovakia*
[c] *Technical University in Zvolen, Faculty of Forestry, T. G. Masaryka 24, 960 53 Zvolen, Slovakia*
[d] *Institute of Forest Ecology of the Slovak Academy of Sciences, Ľ. Štúra 2, 960 53 Zvolen, Slovakia*
[e] *State Forest of TANAP, Tatranská Lomnica, 059 60 Vysoké Tatry, Slovakia*
[f] *USDA Forest Service, Pacific Southwest Research Station, 4955 Canyon Crest Drive, Riverside, CA 92507, USA*

ARTICLE INFO

Keywords:
Ambient ozone
Phytotoxic ozone dose
Stomatal conductance
Site-specific model
Visible O_3 injury

ABSTRACT

Montane forests in the High Tatra Mountains are exposed to high ambient ozone (O_3) concentrations that may adversely affect the physiological processes and health of plants. This study presents the modelled results of the phytotoxic ozone dose (POD) for dwarf mountain pine (*P. mugo*) in 2016. POD metrics were calculated using the deposition model DO_3SE, with O_3 concentration and meteorological data measured in three altitudinal zones. In addition, maximal stomatal conductance (G_{max}) derived from gasometric field measurement in local conditions was included in the model. Field measurements confirmed the robust performance of the DO_3SE model for stomatal conductance (G_{sto}). The site-specific stomatal conductance response model was largely congruent with average values estimated by DO_3SE, though differences in temporal G_{sto} distribution were observed. We determined a moderate limitation of O_3 uptake due to environmental factors (f_{ENVI}) such as air temperature and relative humidity, solar radiation, and soil water availability. It appears that G_{max} is more relevant for annual POD than f_{ENVI} in the temperate mountain forest. The results indicate a high level of POD and O_3 uptake by *P. mugo* in the High Tatra Mountains, which corresponds with the O_3-induced visible injury symptoms observed. We also identified visible O_3 injury in *P. mugo* needles, which was more prevalent among the two-year old needles than younger individuals.

1. Introduction

Surface ozone (O_3) is one of the most common air pollutants that can be harmful to both humans and vegetation (WHO, 2013; EEA, 2017). In recent decades, trends in mean ambient O_3 concentrations varied by region (Cooper et al., 2014); however, they did not appear well correlated with major exposure metrics used for assessing human health or vegetation effects (Lefohn et al., 2017). A variety of O_3 metrics are used in risk assessments of forest trees. The most commonly used O_3 exposure standard (AOT40) is solely based on measured O_3 concentration being > 40 ppb, and fails to account for environmental factors and physiological conditions affecting vegetation responses. Therefore, in late 1990s, a new concept of flux-based critical levels was developed. This advanced approach is based on the principles of O_3 transport from the atmosphere to the plant interior through stomata, and the control of O_3 uptake by leaves via environmental and physiological factors (Fuhrer et al., 1997; Massman et al., 2000; Grünhage et al., 2001; Ashmore et al., 2004; Musselman et al., 2006; Karlsson et al., 2007; Matyssek et al., 2007). A stomatal conductance-based model was also developed to estimate O_3 uptake for a number of the most widespread tree species in Europe (Emberson et al., 2000, 2007; Büker et al., 2012). Flux-based critical levels derived for the phytotoxic ozone dose (POD_Y) (i.e., the accumulated stomatal O_3 flux above detoxification threshold Y) was revised according to the LRTAP Convention (CLRTAP, 2017; Mills et al., 2011). Strong support exists among biologists for the use of threshold O_3 flux that reflects the detoxification capacity of trees (Karlsson et al., 2007; Büker et al., 2015). Expert judgement was used to set $Y = 1\ \mathrm{nmol\ m^{-2}\ PLA\ s^{-1}}$ (where PLA is the projected leaf area) based on observations of O_3 sensitivity under controlled conditions (Dizengremel et al., 2013). A recent study by Feng et al. (2017) revealed that shift from leaf area-based to the leaf mass-based stomatal ozone flux index POD_X (were X is the mass-based flux

Peer review under responsibility of Turkish National Committee for Air Pollution Research and Control.
* Corresponding author.
E-mail address: bicarova@ta3.sk (S. Bičárová).

https://doi.org/10.1016/j.apr.2018.08.003
Received 14 May 2018; Received in revised form 2 August 2018; Accepted 4 August 2018

threshold) significantly simplifies large-scale impact assessments of trees since it potentially allows for one common dose–response relationship for all tree species. However, De Marco et al. (2015) recommend applying POD_Y without the threshold limitation (Y = 0) (i.e., POD_0 rather than POD_1). This approach is based on the fact that all O_3 molecules entering into the leaf may induce a metabolic response (Musselman et al., 2006). Various studies have provided information on how O_3 interacts with plants at the cellular level (Bussotti et al., 2011; Gottardini et al., 2014; Braun et al., 2014). Additionally, the physiological consequences of O_3-induced effects may impair the resistance of trees to abiotic (e.g., frost and drought) and biotic (e.g., nutrient deficiencies, pathogens, and insects) stress factors (Vollenweider and Günthardt-Goerg, 2006).

A major challenge in the development of O_3 standards is their validation against biologically-based field data (Paoletti and Manning, 2007). Recent epidemiological studies have indicated a stronger correlation between POD_0 and visible foliar O_3 injury than for AOT40 (Sicard et al., 2016). The most O_3-sensitive conifers are *Pinus* species e.g. *Pinus halepensis* or *Pinus cembra* in the Mediterranean region (Sicard et al., 2016; Dalstein and Vas, 2005); however, varying visible O_3 injury responses may be expected under specific local conditions (Coulston et al., 2003; Nunn et al., 2007; Braun et al., 2014). Based on a wealth of evidence from the literature, rural and montane areas are exposed to high O_3 concentrations (Bytnerowicz et al., 2004; Hůnová et al., 2010; Zapletal et al., 2012; Adame and Sole, 2013; Bičárová et al., 2016; Nguyen et al., 2017; Kasparoglu et al., 2018). Ozone damage rates increase with altitude in response to increasing O_3 mixing ratios and O_3 uptake due to favourable microclimatic conditions (Díaz-de-Quijano et al., 2009). However, a lack of empirical data concerning vulnerable montane tree species remains.

The objectives of this study were: (i) to map POD_Y ozone metrics (POD_1, POD_0) for the year-round 2016; (ii) to appraise the role of environmental factors in O_3 uptake; and (iii) to analyse the relationship between modelled POD_Y and field observations of visible O_3 injury for dwarf mountain pine (*Pinus mugo* Turra). In order to achieve these goals, we focused on the montane region of the High Tatra Mountains, Slovakia (SK–HT).

2. Study area

The study area (Fig. 1) covers montane forest sites in the SK–HT region, which is situated in the highest mountain range of the Carpathians. The elevation in this region rises from foothills at 800 m a.s.l. to 2655 m a.s.l. at the highest peak. The climate in this area is primarily cold and humid. According to the standard reference climate period (1961–1990), mean annual air temperature ranges from 5.3 °C in the foothills to −3.8 °C above 2600 m a.s.l., while mean annual precipitation varies from 760 to 2000 mm. In the warmer half of the year (Apr–Sep), precipitation reaches nearly 65% of the annual total with the highest amount observed in June or July. This natural coniferous forest is dominated by Norway spruce (*Picea abies* L. Karst), and extends up to 1600 m a.s.l., while the subalpine zone (up to 1800 m a.s.l.) creates a continuous belt and is almost entirely dominated by dwarf mountain pine. In recent decades, the spruce forest has been significantly weakened by long-distance air pollution (Bytnerowicz et al., 2004; Kopáček et al., 2017), heavy windstorms, and bark beetle outbreaks (Mezei et al., 2017) that have reduced forest cover by 50% (Fleischer et al., 2017). Such a drastic reduction in forest area increased the role of dwarf mountain pine in landscape ecological stability in the High Tatra Mountains region, and it remains a species that is relatively undisturbed by abiotic and biotic stress factors. Notably, dwarf mountain pine has been successfully planted outside its natural high mountain biotopes for the provision of various ecosystem services (e.g., slope and water regime stabilisation, greening projects, etc.). In order to map phytotoxic O_3 doses and estimate further functioning of dwarf mountain pine under changing conditions, three study sites distributed in different altitudes were established: foothills (A), submontane (B), subalpine (C) at different aspects (south (sites A, C) and north (site B)). To illustrate O_3 concentration variability in the lower troposphere, we included an additional ground-based O_3 measurement site (D) within the study area, situated at the peak of Lomnický štít (Table 1, Fig. 1).

3. Methods

3.1. Ozone metrics

Stomatal flux-based O_3 metrics (POD_Y) was calculated using the multiplicative deposition model DO_3SE (Büker et al., 2012). An algorithm for model estimation of POD_Y (mmol O_3 m^{-2} PLA) incorporates the effects of meteorological and site conditions such as air temperature (f_{temp}), vapour pressure deficit (f_{VPD}), solar radiation or light (f_{light}), soil water potential (f_{SWP}), plant phenology (f_{phen}), and O_3 concentration (f_{O3}) on maximum stomatal conductance (G_{max}). In the case of coniferous trees, ozone and phenology functions are considered constant

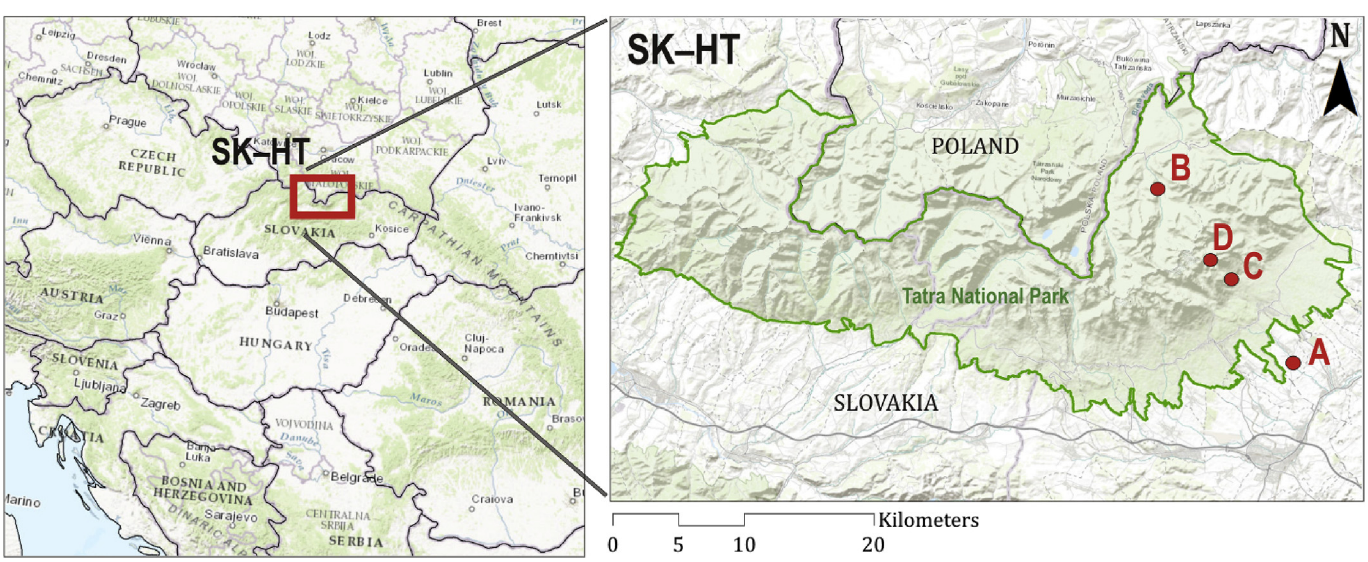

Fig. 1. Geographic position of the study area in the High Tatra Mountains, Slovakia (SK–HT) and location of experimental sites at different altitudes; A – Stará Lesná (810 m a.s.l.); B – Podmuráň (1100 m a.s.l.); C – Skalnaté Pleso (1778 m a.s.l.); D – Lomnický štít (2635 m a.s.l.).

Table 1
Descriptions of experimental sites (using codes from Fig. 1). Long-term average of annual air temperature (AT) and total precipitation (P) data represents the climate period of 1961–1990.

CODE Site name	GPS Latitude Longitude	Altitude Zone/Aspect	$AT_{1961–1990}$ [deg. C]	$P_{1961–1990}$ [mm]	Soil type/Soil texture
A Stará Lesná	49°09′08″ N 20°17′19″ E	810 m a.s.l. Foothill/South	5.3	759	Haplic cambisols/Silt loam (medium coarse)
B Podmuráň	49°15′00″ N 20°09′25″ E	1100 m a.s.l. Submontane/North	4.0	1227	Haplic podzols/Loam (medium)
C Skalnaté Pleso	49°11′21″ N 20°14′02″ E	1778 m a.s.l. Subalpine/South	1.7	1282	Folic leptosols/Sandy loam (coarse)
D Lomnický štít	49°11′43″ N 20°12′54″ E	2635 m a.s.l. Alpine summit	−3.8	1239	Lithic leptosols/Hyperskeletic

(f_{O3} = 1, f_{phen} = 1) due to a moderate senescence-promoting effect on stomatal conductance. The f_{min} function expresses a fraction of G_{max} and represents the relative minimum stomatal conductance occurring during daylight hours.

The passage rate of O_3 entering through the stomata expresses the stomatal O_3 conductance G*sto* (mmol O_3 m^{-2} s^{-1}):

$$G_{sto} = G_{max} * \left[min\left(f_{phen}, f_{O_3}\right)\right] * f_{light} * max\{f_{min}, (f_{temp} * f_{VPD} * f_{SWP})\} = G_{max} * f_{ENVI} \tag{1}$$

Stomatal O_3 flux F_{st} (nmol m^{-2} PLA s^{-1}) is provided by:

$$F_{st} = G_{sto} * c(z_1) * \left(\frac{r_c}{(r_b + r_c)}\right) = G_{max} * f_{ENVI} * c(z_1) * \left(\frac{r_c}{(r_b + r_c)}\right) \tag{2}$$

where $c(z_1)$ is concentration of O_3 (nmol m^{-3}) at the top of the canopy measured in the tree height (z_1), r_b and r_c are the quasi-laminar resistance and leaf surface resistance (s m^{-1}), respectively.

POD_Y is the sum of hourly values of F_{st} (Eq. (2)) over the threshold Y = 1 (POD_1), or without threshold Y = 0 (POD_0), aggregated over the period between the start (SGS) and end (EGS) of the growing season. For conifers, we consider the all seasons period to be from January 1 to December 31. Generally, there is no limitation of stomatal conductance associated with leaf development stage of conifer species (i.e. f_{phen} = 1), stomatal O_3 flux is driven particularly by air temperature defined according to the f_{temp} function (CLRTAP, 2017).

$$POD_Y = \sum_{SGS}^{EGS} (F_{st} - Y) * (3{,}600/10^6) \tag{3}$$

The stomatal flux-based critical level ($CLef_1$) of POD_1 was set to a value of 9.2 mmol O_3 m^{-2} PLA for an acceptable biomass loss of forest trees, especially Norway spruce (CLRTAP, 2017). An innovative species-specific CLef of POD_0 is proposed to be 19 mmol O_3 m^{-2} PLA for forest protection against visible O_3 injury for highly O_3-sensitive pine species (Sicard et al., 2016). The manual for modelling and mapping critical level exceedance provides a more specific description of the algorithm and derivation of physical relationships for the final calculation of POD_Y (CLRTAP, 2017). In this work, the pre-set, built-in version (3.0.5) of the DO_3SE model available at http://www.sei-international.org/do3se, with the collection of parameters for coniferous forests (CF), was used (Table S1). Maximal stomatal O_3 conductance G_{max} (mmol O_3 m^{-2} PLA s^{-1}), as key parameter of stomatal O_3 flux (Eq. (2)) in dwarf mountain pine, was obtained from field experiments (Fig. 2a). For the calculation of POD at each study site, the model requires measured hourly O_3 and meteorological data.

3.2. Ozone and meteorological data

Ozone concentration was measured by active monitors (Horiba–APOA360, Thermo Electron Environmental 49C, and 2B Tech Ozone Monitor M106-L) based on UV absorption by O_3 at a wavelength of 254 nm. Hourly mean data at three experimental forest stands (A, B, C) were continuously recorded without major gaps during 2016. Furthermore, O_3 concentrations measured at the Lomnický štít site (D) were used to illustrate O_3 variability at different altitudes (810–2635 m a.s.l.). Meteorological variables were continuously monitored at all experimental sites using the measurement system based on a PROlog ultra-low power datalogger (Physicus, SK). The following identical sensors were used for measurements at all sites: a temperature probe with platinum resistance thermometers Pt100 for air temperature (at 2 m above the surface); Prove-HumiAir 9 for relative air humidity; Pyranometer CMP3 (Kipp and Zonen) for global solar radiation; Wind Transmitter Compact (Thies Clima) for wind speed, PressAir sensor for air pressure, and a Rain Gauge (MR3H – Meteoservice CZ) for precipitation. Selected meteorological data allowed for specification of the environmental functions associated with air temperature (Eq. (4)), vapour pressure deficit (Eq. (5)), and irradiance radiation and light (Eq. (6)):

$$f_{temp} = max\left\{f_{min}, \left[\left(\frac{AT - T_{min}}{T_{opt} - T_{min}}\right) * \left(\frac{T_{max} - AT}{T_{max} - T_{opt}}\right)\right]^{\left(\frac{T_{max} - T_{opt}}{T_{opt} - T_{min}}\right)}\right\} \tag{4}$$

$$f_{VPD} = min\left\{1, max\left[f_{min}, \left((1 - f_{min}) * \left(\frac{VPD_{min} - VPD}{VPD_{min} - VPD_{max}}\right)\right) + f_{min}\right]\right\} \tag{5}$$

$$f_{light} = 1 - EXP((-light_a) * PFD) \tag{6}$$

where AT is measured air temperature (°C); VPD is vapour pressure deficit (kPa) calculated on base of measurement of air temperature and relative air humidity; PFD represents the photosynthetic photon flux density in units of μmol m^{-2} s^{-1} i.e., photosynthetically-active radiation (PAR) derived from measurement of global solar radiation R (W m^{-2}). These variables are complete with the species-specific parameters f_{min}, T_{min}, T_{opt}, T_{max}, VPD_{min}, VPD_{max}, and $light_a$ (listed in Table S1). The functions f_{temp}, f_{VPD}, and f_{light} are expressed in relative terms (i.e., they accept values between 0 and 1 as a proportion of G_{max}).

3.3. Soil water potential

Soil moisture data were obtained by two approaches: field measurements and modelling. Both real-time and modelled soil water potential (SWP) data were useful for specification of the f_{SWP} function (Eq. (7)).

$$f_{SWP} = min\{1, \{f_{min}((1 - f_{min}) * (SWP_{min} - SWP)/(SWP_{min} - SWP_{max})) + f_{min}\}\} \tag{7}$$

The f_{SWP} function defines the effect of soil moisture on G_{sto} (Eq. (1)) in relative terms, similar to the aforementioned functions (Eqs. (4)–(6)). Additional parameters, such as f_{min}, SWP_{min}, SWP_{max}, are listed in Table S1. Differences between f_{SWP} based on measured and modelled SWP allow to evaluate the reliability for the soil moisture module included in the DO_3SE model. This modelling approach incorporated hydraulic resistance (steady state, SS) to water flow through the plant system

(Büker et al., 2012). Field measurement of SWP was conducted at three soil depths (−0.1, −0.2, −0.4 m) at all experimental sites (except site D – Lomnický štít). SWP values were measured using gypsum blocks at a range of up to −1.5 MPa (GB2, Delmhorst Instrument, U.S.A.). SWP data were stored in integrated data loggers (MicroLog SP3, EMS Brno, CZ) at 1-h intervals.

3.4. Maximum level of stomatal ozone conductance

Data on maximum stomatal conductance or the general response of dwarf mountain pine stomata to environmental factors remains relatively sparse in the literature. A review by Hoshika et al. (2018) which summarized the G_{max} data for plant functional types showed a range of G_{max} from 0.07 to 0.36 (mmol H_2O m^{-2} s^{-1}) in woody plants. Maximal stomatal conductance (G_{max}, mmol O_3 m^{-2} PLA s^{-1}) is a key parameter (Eq. (1)) for calculation of stomatal O_3 flux in the DO_3SE model (Eq. (2)). In this study, data needed to specify of the G_{max} for dwarf mountain pine were obtained by direct measurement. For this purpose the LI-6400 photosynthesis system (Li-Cor, Inc., Lincoln, NE) equipped with a standard Licor 6400-22 Opaque Conifer Chamber and 6400–18 RGB Light Source was used. To capture a wide range of environmental conditions, we measured stomatal conductance from June to November at two study sites situated at different elevations: site A (Stará Lesná, 810 m a.s.l.) and site C (Skalnaté Pleso, 1778 m a.s.l.). During the experiment, internal chamber temperature ranged from 5 to 35 °C, VPD from 0.2 to 3.5 kPa, photosynthetic photon flux density (PPFD) from 0 to 2500 μmol photons m^{-2} s^{-1}, and CO_2 concentration was set to 400 ppm. Prior to each measurement, gas exchange was permitted to stabilise for approximately 6–10 min. Gas exchange measurements were conducted frequently on the attached sunlit terminal shoots of lateral branches from the middle part of plants that appeared healthy. On average, eight to nine measurements per shoot were recorded under various conditions. We considered G_{sto} (mmol O_3 m^{-2} PLA s^{-1}) from G_{sto} (mmol H_2O m^{-2} PLA s^{-1}) using a conversion factor of 0.663 (Massman, 1998) to account for the difference in the molecular diffusivity of water vapour (measured by LI-6400 photosynthesis system) to that of ozone. Maximum stomatal conductance G_{max} was derived as the 95th percentile of all measured data on stomatal conductance for O_3 flux rates (approximately 2700 total measurements of G_{sto}) after removal of outliers. Based on this derivation, the maximum level of stomatal O_3 conductance for dwarf mountain pine was determined to be G_{max} = 110 mmol O_3 m^{-2} PLA s^{-1} (Fig. 2a).

In order to verify the performance of G_{sto} in the DO_3SE model, we developed a site-specific stomata response function (Eq. (8)) for dwarf mountain pine using the symbolic regression approach. HeuresticLab ver. 3.13 software (Wagner et al., 2014) processed 2400 readings of G_{sto} (marked as “Measured” in Fig. 2b) and wide spectrum of environmental variables (air temperature, leaf temperature, VPD, CO_2 concentration, RH, PAR, air pressure, SWP, and soil moisture and temperature). Two-thirds of G_{sto} data from the field (1600 measurements randomly selected) were included for model development (marked as “Training” in Fig. 2b), and one-third of this data (800 measurements) were included for an evaluation of model performance (marked as “Test” in Fig. 2b). The final simplified and optimised model based on two variables (AT – air temperature and VPD – vapour pressure deficit) was as follows:

$$Gsto = \left(\frac{AT*log(c_0*AT + c_1)*c_2}{c_3*VPD}\right) + c_4 \tag{8}$$

with parameters: $c_0 = 1.9854$, $c_1 = -16.34$, $c_2 = 0.16571$, $c_3 = 267.39$ and $c_4 = 0.01287$.

A test of response function (Eq. (8)) produced reliable G_{sto} results. Moreover, the relationship between the measured and tested values of G_{sto} was characterised by a coefficient of determination (R^2) of 0.63, Pearson correlation coefficient (R) of 0.79, a mean absolute error (MAE) of 7.7 mmol O_3 m^{-2} s^{-1}, and an average relative error (ARE) of 10%.

3.5. Visible ozone injury

In November 2016, observations of visible injury symptoms on dwarf mountain pine needles were performed in accordance with the recommended methods for analysis of air pollution effects on forests (CLRTAP, 2017). We evaluated the branches of dwarf mountain pine sampled from eleven plots situated along an altitudinal profile (from 800 to 2000 m a.s.l.). At each plot, we selected five sample trees exposed to sunlight. For each tree, 5 branches with at least 30 needles per needle age class (current year foliage (C), one-year old (C+1), and two-year old needles (C+2)) were removed from the upper third of the crown. For each branch, the percentage of total needle surface affected by visible foliar O_3 injury for C, C+1 and C+2 was scored. Finally, the mean percentage of needle surface affected by visible foliar O_3 injury was calculated for each plot.

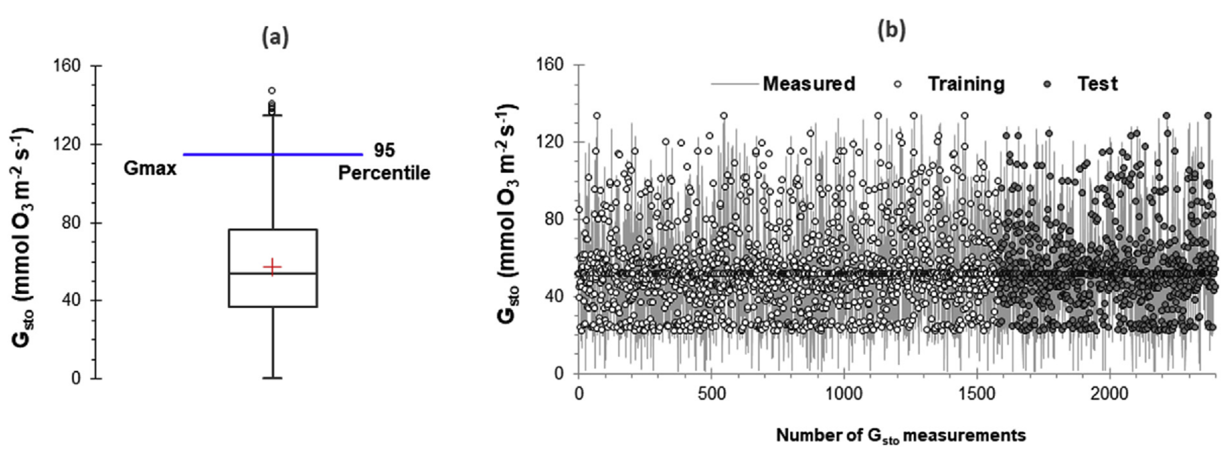

Fig. 2. Stomatal conductance (G_{sto}) for dwarf mountain pine in SK–HT: (a) box plot of measured data and the derived parameter G_{max}; (b) comparison of G_{sto} measured by Licor6400XT and tested by a site-specific regression function (Eq. (8)).

Table 2
Statistics of hourly O_3 and meteorological data in different altitude zones during 2016.

Variables	Statistics	A	B	C	D
O_3 concentration	O_3 (ppb)				
	Mean	28.7	29.6	45.9	48.5
	Max	64.0	68.6	81.2	86.0
	Min	2.3	1.7	10.0	15.7
	STD	11.7	13.8	9.1	8.7
	Var. Coeff. (%)	40.8	46.6	19.8	17.9
Air temperature	AT (°C)				
	Mean	6.5	5.0	3.0	−3.2
	Max	29.9	27.8	23.1	16.6
	Min	−18.9	−20.1	−18.7	−22.5
	STD	8.9	8.2	7.5	7.5
	Var. Coeff. (%)	136.9	164.0	250.0	234.4
Vapour pressure deficit	VPD (kPa)				
	Mean	0.27	0.17	0.19	0.12
	Max	2.30	1.80	1.56	1.60
	Min	0.02	0.01	0.02	0.00
	STD	0.33	0.24	0.18	0.18
	Var. Coeff. (%)	122.2	141.2	94.7	150.0
Precipitation	P (mm)				
	Mean	0.08	0.18	0.18	0.39
	Max	37.6	28.6	27.6	71.2
	Sum	727	1545	1601	2277
	STD	0.61	0.91	0.80	0.49
	Var. Coeff. (%)	762.5	505.6	444.4	125.6
Global solar radiation	R (kW m^{-2})				
	Mean	0.13	0.10	0.12	0.13
	Max	1.03	1.01	1.15	0.97
	Sum	1133	900	1068	1136
	STD	0.22	0.20	0.20	0.20
	Var. Coeff. (%)	169.2	200.0	166.7	153.8

4. Results

4.1. Variability of O_3 concentration and meteorological data

As expected, mean annual O_3 concentrations throughout 2016 (Table 2) increased with altitude from 28.7 ppb (A) to 48.5 ppb (D). Relatively high O_3 concentration (Fig. 3), favourable meteorological conditions (Fig. 4), and sufficient soil moisture (Fig. 5) suggest high levelof stomatal O_3 uptake by timberline vegetation of the subalpine (C) and alpine (D) zone. Monthly mean of O_3 concentration varied between 20 ppb and 40 ppb from the foothill (A) up to submontane (B) zone, while the subalpine (C) and alpine zones experienced concentrations above 40 ppb (D). Monthly O_3 means peaked in May (Fig. 3b), and achieved values between 36.3 ppb (B) and 59 ppb (D). Diurnal variation of hourly O_3 concentration (Fig. 3c) at lower altitudes (A, B) clearly contrasted with relatively stable concentrations at higher elevations (C, D). Daytime hourly mean O_3 concentration varied between 20 and 40 ppb for the foothill and submontane zone, while higher altitudes experienced fluctuations approaching 50 ppb at all hours of the day. These high O_3 concentrations occurred in the cold and humid climates of the subalpine and alpine zones, where annual mean air temperatures were 3.0 °C and −3.2 °C, respectively (AT, deg. C in Table 2). Annual mean values and the maxima of vapour pressure deficit (VPD, kPa) suggested air humidity conditions favourable for unlimited stomatal conductance at all plots (Table S1). Precipitation totals (P, mm) between 1545 mm and 2277 mm ensured a sufficient supply of soil water for the roots of dwarf mountain pine from submontane to alpine zones. Global solar radiation (R, kW m^{-2}) measurements confirmed the assumption of lower values for total solar irradiance existing on the north exposure site (B) in comparison to plots situated on southern portion of the SK–HT. Statistical significance of variability of meteorological parameters and O_3 concentration from different localities was assessed by one-way ANOVA with Fisher LSD post-hoc test. Test showed significant differences ($p > 0.05$) in all variables except precipitation between C and B site. The coefficients of variation (Var. Coeff.) in Table 2 as a relative indicator of variability of each variable show evidently lower dispersion in O_3 concentration than for meteorological variables. This underlines the role of meteorological conditions in O_3 uptake.

4.2. Response of stomatal conductance to environmental factors

The relationship between meteorological factors f_{temp}, f_{VPD}, f_{light} (Eqs. (4)–(6)), derived from the measurements (Table 2) and stomatal conductance G_{sto} (Eq. (1)), is illustrated in Fig. 4. As expected, a relatively cool and humid mountain climate in SK–HT did not limit G_{sto} due to the absence of extremely high air temperatures ($> T_{max}$) as well as low air humidity ($> VPD_{min}$). With the exception of frosty days during the winter season (Nov–Mar), air temperatures typically varied between T_{min} and T_{opt}, and the frequency of air temperatures higher than T_{opt} decreased from the foothills (A) to the subalpine zone (C). Similarly, VPD values above VPD_{max} were more frequently recorded on foothills (A) when compared to higher elevation sites (B, C). Solar light conditions characterised by photosynthetically-active radiation (PAR) were similar among south-exposed plots (A, C). Although the northern plot (B) received slightly less solar energy (Table 2), f_{light} values associated with PAR were not substantially different. Upper values of G_{sto} achieved levels of 90 mmol O_3 m^{-2} s^{-1} if the measurement-based parameter G_{max} = 110 mmol O_3 m^{-2} s^{-1} (Fig. 2a)

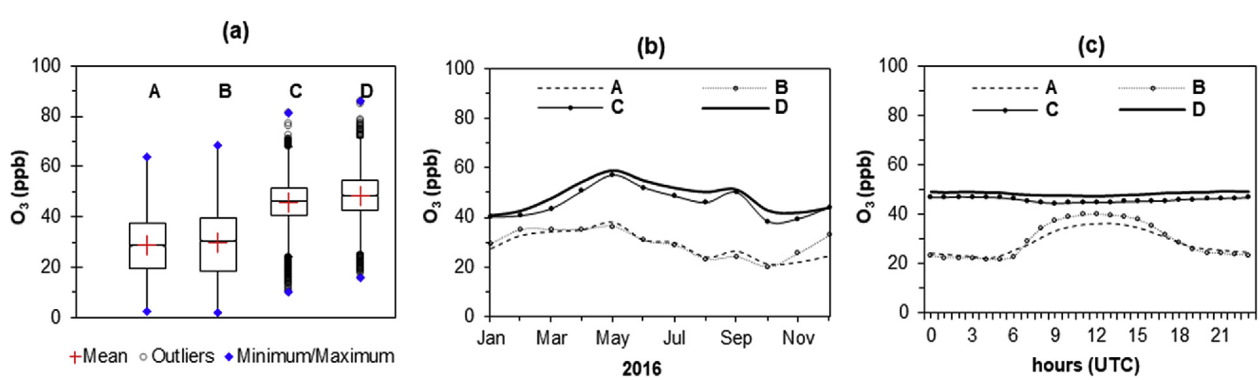

Fig. 3. Variability of hourly O_3 concentrations (ppb): (a) mean annual data, (b) mean monthly data, and (c) diurnal variation at different altitudes (A, B, C, D) over 2016.

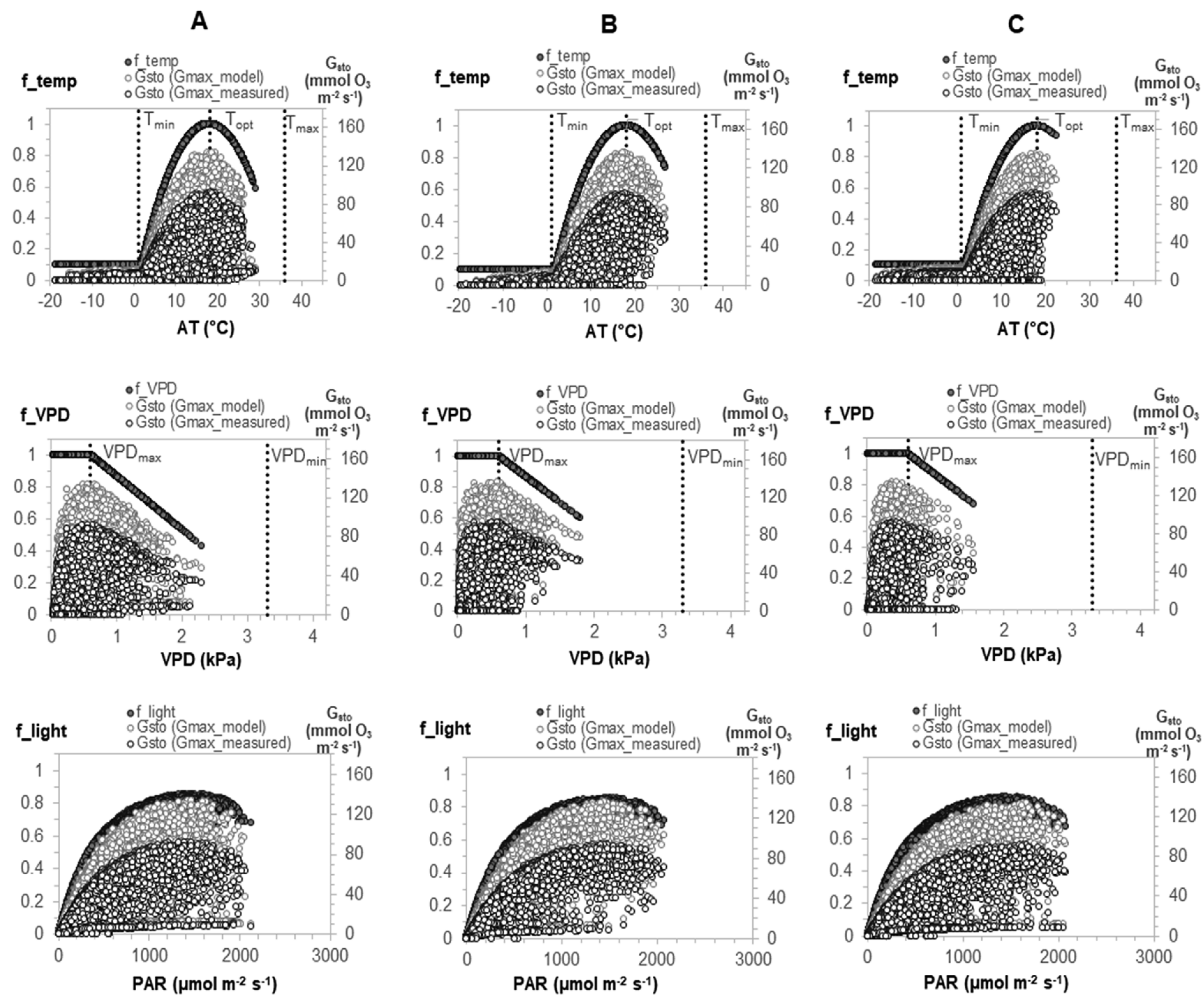

Fig. 4. Air temperature (AT, deg. C), vapour pressure deficit (VPD, kPa), and photosynthetically-active radiation (PAR, µmol m^{-2} s^{-1}) in relation to environmental factors (f_temp, f_VPD, and f_light) and model results for G_{sto} (mmol O_3 m^2 s^{-1}) according to the G_{max} parameter as a pre-set value in model (G_{sto}:G_{max}_model) and field measurement in local conditions (G_{sto}:G_{max}_measured) for different altitudes (A, B, and C); dotted vertical lines depict the variable ranges (AT, VPD) for effective stomatal O_3 conductance (Table S1).

was considered. In the model-based G_{max} = 160 mmol O_3 m^{-2} s^{-1} (Table S1), upper values of G_{sto} were approximately 20% higher, and achieved a maximum level of 130 mmol O_3 m^{-2} s^{-1}. This difference suggests that the value of G_{max} may have a more pronounced effect on the results of G_{sto} than other environmental factors related to air temperature (AT, deg. C), vapour pressure deficit (VPD, kPA), photosynthetically-active radiation (PAR, µmol m^{-2} s^{-1}), and soil water potential (SWP, MPa).

The effect of soil moisture regime on G_{sto} was analysed according to modelled and measured SWP values and the f_{SWP} function (Eq. (7)). In submontane (B) and subalpine zones (C), differences between SWP values modelled via DO_3SE and SWP were negligible with respect to effective intervals SWP_{min} and SWP_{max} (Fig. 5). A f_{SWP} value of 1 confirms the assumption of soil moisture at higher altitudes being sufficient for unlimited stomatal conductance and O_3 uptake. However, at the foothill site (A), differences between modelled and measured SWP and f_{SWP} were larger. During warm months (May–Aug), modelled results and measured SWP values decreased to minimal levels of −2.0 MPa and −1.3 MPa, respectively. In addition, SWP measurements indicate that soil water drought events (SWP < SWP_{max}) also occurred in autumn (Sep–Oct) and winter (Jan), while modelled values varied by approximately −0.1 MPa during these periods. As such, it appears that the model generates results inconsistent with SWP measurements for the foothill zone (A).

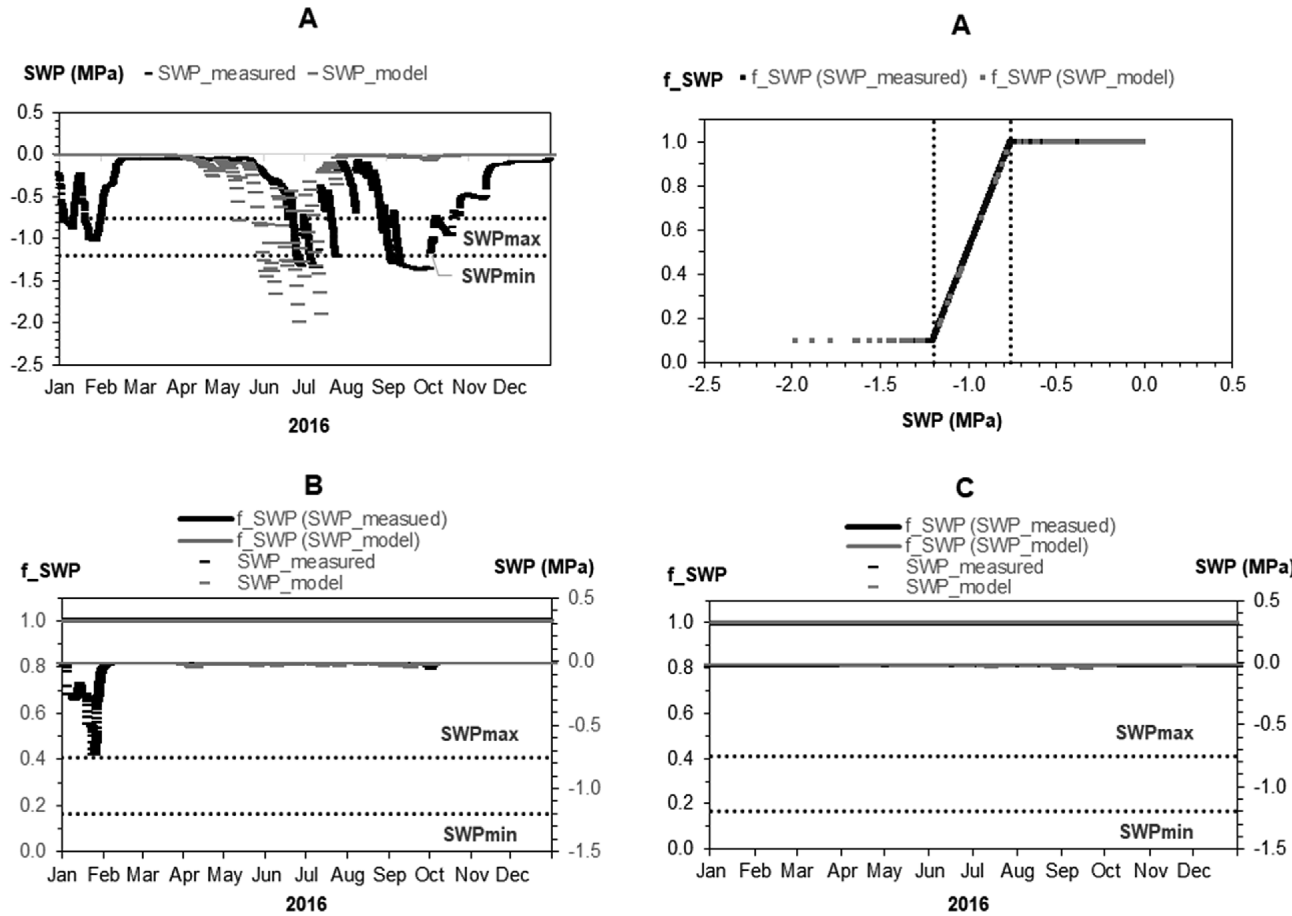

Fig. 5. Soil water potential (SWP, MPa) and factor f_SWP (Eq. (7)): comparison between measured and modelled values for different altitudes (A, B, and C) in 2016; dotted lines illustrate SWP ranges for effective stomatal O_3 conductance (Table S1). Stomatal conductance calculated by the DO_3SE (Eq. (1)) and site-specific model (Eq. (8)) were compared at three study sites (A, B, and C).

In order to use comparable datasets for the evaluation of G_{sto} based on the DO_3SE model (Eq. (1)) and site-specific model (Eq. (8)), some data were excluded from the assessment. Due to erroneous instrument (LI-6400) responses below 5 °C and unreliable measurements below 8 °C (chaotic stomata behaviour), only data exhibiting AT above 9 °C were chosen for comparison (approximately 3% data were excluded). The second criterion for data reduction was low PAR (around 8%), which was due to slow stomatal response to PAR below 150 μmol m^{-2} s^{-1} and rapid change in VPD. On average, stomatal adaptation to changing light conditions in gasometer chamber lasted nearly 40 min. Thus, to keep other environmental parameters constant in field conditions was nearly impossible. Notably, according to gasometric measurement, PAR values above 150 μmol m^{-2} s^{-1} did not noticeably control stomatal conductance, which explains why PAR did not appear in the site-specific model. Stomatal conductance for O_3 uptake by dwarf mountain pine estimated by the DO_3SE and site-specific models for the three study sites is presented in Fig. 6. The average values of stomatal conductance estimated by two models were similar at all three sites. Moreover,

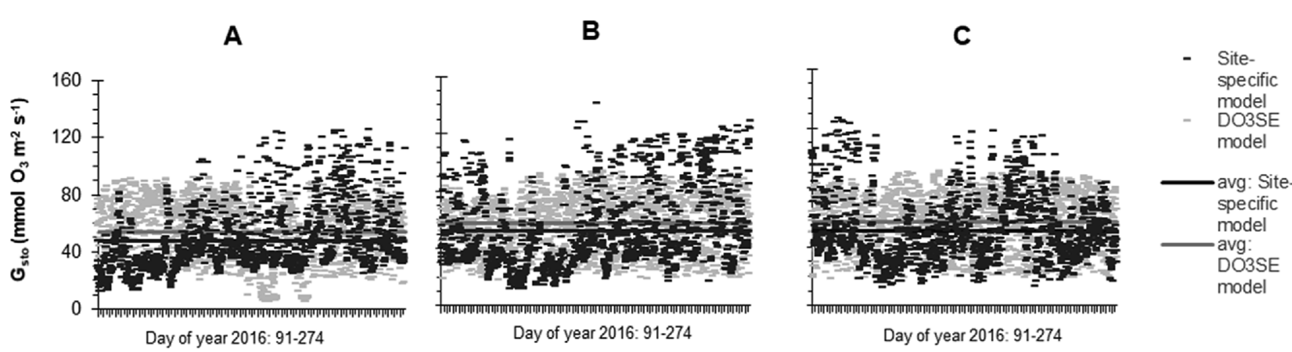

Fig. 6. Stomatal conductance (G_{sto}; mmol O_3 m^{-2} s^{-1}) according to the DO_3SE (Eq. (1)) and site-specific model (Eq. (8)) estimated for selected meteorological conditions (AT above 9 °C and PAR above 150 μmol m^{-2} s^{-1} from April 1st to September 30th (DOY 91–274) for dwarf mountain pine at three study sites (A, B, and C) in SK–HT.

Table 3
DO_3SE model outputs for POD_1 and POD_0 ozone metrics.

Site code	Y = 0 Y = 1	POD_Y (mmol O_3 m^{-2} PLA)					POD_Y (mmol O_3 m^{-2} PLA)				
		M1: measured G_{max} = 110 mmol O_3 m^{-2} s^{-1} (Fig. 2)					M2: model G_{max} = 160 mmol O_3 m^{-2} s^{-1} (Table S1)				
		f_{ENV} (Eq. (1))					f_{ENV} (Eq. (1))				
		R_ real	MS_model simulation f_{ENVI}				R_ real	MS_model simulation f_{ENVI}			
		f_{ENVI}	f_{temp} = 1	max_f_{light}	f_{VPD} = 1	f_{SWP} = 1	f_{ENVI}	f_{temp} = 1	max_f_{light}	f_{VPD} = 1	f_{SWP} = 1
A	POD_0	19.1	24.9	20.6	19.6	19.9	23.3	30.2	25.0	23.6	26.4
B	POD_0	19.9	27.9	21.3	20.4	19.9	26.6	37.0	28.6	27.2	26.6
C	POD_0	22.1	38.3	23.0	22.3	22.1	30.6	52.5	31.8	30.8	30.6
A	POD_1	8.4	11.8	9.0	9.1	8.9	12.2	16.9	13.0	12.8	14.6
B	POD_1	10.3	15.0	10.6	10.8	10.3	16.1	23.4	16.9	16.7	16.1
C	POD_1	11.6	23.6	11.8	11.8	11.6	19.2	37.5	19.6	19.3	19.2
	POD_Y ratio		f_{ENVI} (MS: R)				G_{max} (M2: M1)	f_{ENVI} (MS: R)			
A	POD_0	:	1.30	1.08	1.03	1.04	1.22	1.30	1.07	1.01	1.13
B	POD_0	:	1.40	1.07	1.03	1.00	1.34	1.39	1.08	1.02	1.00
C	POD_0	:	1.73	1.04	1.01	1.00	1.38	1.72	1.04	1.01	1.00
A	POD_1	:	1.40	1.07	1.08	1.06	1.45	1.39	1.07	1.05	1.20
B	POD_1	:	1.46	1.03	1.05	1.00	1.56	1.45	1.05	1.04	1.00
C	POD_1	:	2.03	1.02	1.02	1.00	1.66	1.95	1.02	1.01	1.00

temporal variation was more pronounced all sites differences. Generally, stomatal conductance interpreted using DO_3SE was more flattened compared to the site-specific model.

4.3. Phytotoxic ozone dose and stomatal O_3 uptake

The DO_3SE model results (Table 3) indicate increasing stomatal O_3 uptake in dwarf mountain pine from foothills (A) to the subalpine zone (C), which corresponds with a rise in O_3 concentration along altitudinal zones (Fig. 3a) and an appropriate environmental conditions for stomatal O_3 flux (Fig. 4). Accumulated stomatal O_3 flux without a threshold (Y = 0), POD_0, ranged from 19.1 to 22.1 mmol O_3 m^{-2} PLA if environmental factors were considered (R_f_{ENVI}) and maximal stomatal conductance (M1_G_{max} = 110 mmol O_3 m^{-2} s^{-1}) was derived from the field measurements. These values are approximately 22–38% lower in comparison to POD_0 based on the pre-set model parameter (M2_G_{max} = 160 mmol O_3 m^{-2} s^{-1}). Model simulation of environmental factors MS_f_{ENVI} suggests weak growth of POD_Y (up to 5%) in conditions entirely unlimited by VPD (f_{VPD} = 1), PAR (f_{light} = 1), and SWP (f_{SWP} = 1) at higher altitudes (B, C). Simulation of wet soil conditions (f_{SWP} = 1) in foothills, where real soil drought events occurred, could lead to alter POD_Y levels by up to 20%. The highest increase in POD_Y (30–103%) resulted from simulations considering optimal air temperature conditions (f_{temp} = 1). This simulation suggests the possibility of a further rise of POD_0 in relation to the effect of global warming. Modelled POD_0 values exceeded critical level for highly O_3-sensitive pine conifers (CLef = 19 mmol m^{-2} PLA) at all plots (A, B, and C). Phytotoxic ozone dose with a threshold Y = 1 (POD_1) varied from 8.4 to 11.6 mmol O_3 m^{-2} PLA. Although the critical level of POD_1 for dwarf mountain pine yet to be determined, an exceedance $CLef_1$ (9.2 mmol O_3 m^{-2} PLA) proposed for Norway spruce was observed in plots B and C, representing the forest belt between the submontane and subalpine zones, where dwarf mountain pine naturally occurs.

4.4. Visible ozone injury

Dwarf mountain pine branches sampled along the vertical profile from 800 to 2000 m a.s.l. exhibited obvious visible O_3 injury at higher altitudes (Fig. 7). More pronounced visible symptoms were observed for two-year old needles (C + 2) at 18.2 ± 2.3% than one-year old needles (C + 1) at 7.7 ± 1.1%. For all plots, the oldest needles were damaged by O_3 more frequently than younger ones. We did not observe signs of foliar senescence on assessed needles. Senescence begins in mid-August in needles of the oldest age classes (Nebel and Matile, 1992). The youngest (current year) needles did not show any chlorotic mottle or marbling, which are characteristic markers of O_3 damage. Additionally, no differences were observed between southern and northern exposures. Higher percentage of visible O_3 symptoms could be caused by a mild winter in 2015/2016, with unusually low snow cover in throughout SK–HT plots. The dwarf mountain pine vegetation, which is usually covered by snow in spring, was exposed to high concentrations of ambient O_3 from February to May 2016 (Fig. 3b). Trend lines (Fig. 7) show an increase in POD_0 and percentage of visible O_3 injury with increasing altitude. This observation confirms that dwarf mountain pine is sensitive to ozone, making it an appropriate conifer species for further monitoring of O_3 phytotoxic effects in the SK–HT.

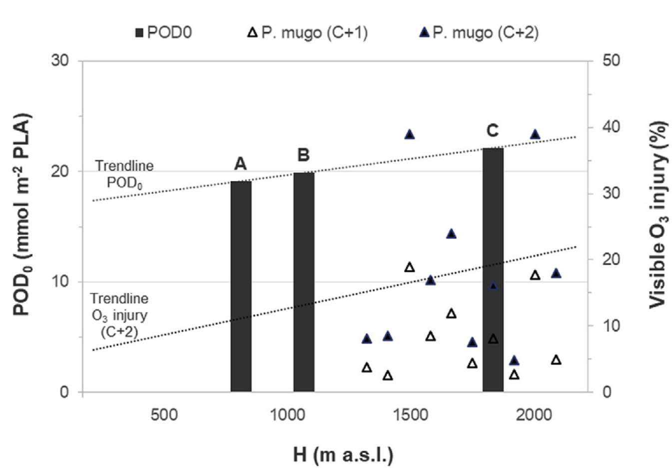

Fig. 7. POD_0 at different altitudes (A, B, C) and percentage of visible O_3 symptoms on needles of different age (C + 1, C + 2) for dwarf mountain pine in the SK–HT.

5. Discussion

Evaluation of the phytotoxic effect of ozone on coniferous trees at high elevation and vulnerable mountain forests necessitates a special approach. Model simulations of stomatal O_3 uptake require continuous field measurements of hourly O_3 concentration and various additional meteorological parameters. Precise parameterisation of the DO_3SE model is also important for the calculation of accumulated stomatal O_3 flux (i.e., POD_Y metrics). Such data is widely available for some commonly occurring trees species, such as Norway spruce (Mills et al., 2011; CLRTAP, 2017), which exhibits with low sensitivity to O_3 exposures (Coulston et al., 2003). However, a paucity of empirical data exists concerning potentially vulnerable mountain forest tree species. Therefore, modification of input parameters reflecting the real environmental conditions of specific coniferous species would be particularly useful. In this regard, we suggest that maximal stomatal conductance of mountain pines is especially important.

In the present study, we modified maximal stomatal conductance (G_{max} = 160 mmol O_3 m^{-2} PLA s^{-1}), which is generally used in the DO_3SE model, as a standard for coniferous tree species. Based on real-time measurements of mountain pines in SK–HT, we altered this pre-set value to G_{max} = 110 mmol O_3 m^{-2} PLA s^{-1} (Table S1). This modification resulted in POD_Y values being substantially lower (22%–64%) than those predicted by the DO_3SE model with the pre-set G_{max} value. For this reason, we recommend that field measurements of stomatal conductance be performed for determination of the correct G_{max} corresponding to local environmental conditions for selected tree species. Similarly, local parameterisation of environmental functions f_{ENVI}, including the effects of meteorological factors and soil moisture on stomatal conductance G_{sto} (Eq. (1)), should be useful for verification of results from the DO_3SE model.

It is necessary to consider some degree of uncertainty in the DO_3SE model when simulating stomatal function, which is primarily driven by soil water potential. In the present study, inconsistency between modelled and measured SWP (Fig. 5) for foothills (A) underline the necessity for including site-specific real-time SWP data into the DO_3SE model. However, studies such as that of Büker et al. (2015), experimentally-induced soil water stress was not found to substantially reduce POD_Y, which was primarily due to the short duration of the soil water stress periods. For a significant reduction of stomatal conductance (and resultant O_3 fluxes), longer episodes of reduced water availability are needed. Since a sufficient amount of precipitation (Table 2) and soil water (Fig. 5) is available for unlimited stomatal O_3 uptake in submotane (B) and subalpine (C) zones, we can confirm that in the upper montane forests (SK − HT) the SWP effect (Eq. (7)) on G_{sto} (Eq. (1)) to become negligible (f_{SWP} = 1) for the POD_Y calculation (Eq. (2)). Moreover, the largely cold and humid climate caused the meteorological factors f_{temp} (Eq. (4), Fig. 5) and f_{VPD} (Eq. (4), Fig. 5) not to reduce O_3 uptake by preventing the effects of very hot and dry weather at higher altitudes. The effect of air temperature on stomatal O_3 conductance tested by the model simulation for T_{opt} (Table S1) shows larger theoretical values of POD (30–203%) compared to actual conditions (Table 3). Although we cannot expect such steep changes of air temperature in the subalpine zone in the near future, increasing O_3 uptake associated with global warming is assumed. According to data collected at the meteorological observatory at Skalnaté Pleso, annual average air temperature fluctuated around the long-term average for the 1941–1991 period (1.8 °C). However, average annual temperature was already 3.1 °C during 2004–2015, and reached maximum values of ~4 °C by the end of this period (Kopáček et al., 2017).

Furthermore, our study revealed the importance of nocturnal plant transpiration and stomatal conductance for more precise estimation of POD_o values. The DO_3SE model sets night-time values to zero, thus underestimating nocturnal stomatal conductance. The preliminary night-time physiological measurements on dwarf mountain pine from this study (unpublished data) indicate the potential importance of nocturnal fluxes, as in other tree species (Zeppel et al., 2013; Hoshika et al., 2018).

A study by Büker et al. (2015) indicated the possibility to define dose–response relationships both by species and by plant functional types, and that the use of a simplified parameterisation of the stomatal conductance model can provide a reasonable accuracy in the calculation of PODy for non-Mediterranean tree species. Our study confirms good performance of the DO_3SE model in specific local conditions with regards to stomatal conductance G_{sto}. We confirmed the reliable estimation of G_{sto} by direct gasometric measurements (Fig. 6) and developed a site-specific stomatal response function (Eq. (8)). Differences between the two models at three study sites were below 12%. However, temporal variation exhibited notable differences. Contrary to the relatively flattened DO_3SE results, stomatal conductance from the site-specific model was notably more sensitive to environmental variables. At this stage, we cannot conclude if divergence in model predictions would yield different POD, especially in coniferous species with less pronounced phenology.

Based on the results of our study, we can confirm that visible O_3 injury increases with rising altitude (Díaz-de-Quijano et al., 2009; Kefauver et al., 2014). Moreover, O_3 concentrations and O_3 uptake in foliar tissues rise with altitude is supported by many previous studies (Chevalier et al., 2007; Bičárová et al., 2016). A relatively high percentage of visible O_3 injury observed on *P. mugo* may be related to specific micro-site conditions for growth (Coulston et al., 2003; Nunn et al., 2007; Braun et al., 2014). Recently utilised methods for evaluation of O_3 injury symptoms in conifers have produced some questionable results, as discussed by several authors (e.g., Wieser et al., 2006). Ozone-induced visible injury related to oxidative stress does not leave any elemental residues that can be detected by analytical techniques. Other abiotic and biotic factors can mask ozone effects, therefore complicating response interpretation. The assessment of O_3 visible injury, in combination with measured O_3 concentration and modelled O_3 uptake, represents a valuable tool for the estimation of potential risk from ambient O_3 in European forest ecosystems (ICP, 2017). Within our study, a dose-response relationship was supported in Fig. 7, showing similar trend lines both for ozone visible injury and POD_0. Obvious visible symptoms associated with high O_3 uptake in dwarf mountain pine suggests a high potential risk of O_3 pollution for the subalpine ecosystems in SK–HT. In addition, widespread spatial distribution of *P. mugo* and its closely related species *P. uncinata* or *P. rotundata* in European mountains (Kefauver et al., 2014) provides opportunity to consider dwarf mountain pine as the subject of further research activities focused on biomonitoring of O_3 injury in the montane environment.

6. Conclusions

The results of the present study confirm expected increases in O_3 concentrations, O_3 uptake, and phytotoxic ozone dose (POD) with increasing altitudes. Model values of POD_0 exceeded the critical level for highly O_3-sensitive pine species at all experimental plots, where field measurements of O_3 concentration and meteorological data processed in model were conducted during 2016. Environmental factors reflecting air humidity and soil moisture conditions allow nearly unlimited capture of O_3 in conifer needle tissues in areas between the submontane and subalpine zone. In foothills, we observed a reduction in O_3 uptake as a response to acute soil moisture deficit during the summer season (June–July). However, validation of modelled against measured values of soil water potential (SWP) showed inconsistencies. This is significant, as modelling of stomatal O_3 flux must consider SWP field measurements, particularly in areas where soil drought events occur. The effect of air temperature on stomatal O_3 conductance corresponds with the relatively cold climate of the High Tatra Mountains. Model simulation considering optimal air temperature conditions suggests higher O_3 uptake associated with global warming. According to field measurements, we modified key a parameter (i.e., maximal stomatal conductance G_{max}) for adaptation to local environmental conditions. This modification resulted in substantially lower POD_0 values (22–66%) than those predicted by the DO_3SE model, with pre-set G_{max} generally being used as a standard for coniferous tree species. Field observations of O_3-induced visible injury on dwarf mountain pine confirmed that older needles were more damaged by O_3 than younger ones. The incidence of visible O_3 symptoms is consistent with the measured O_3 concentration and modelled values of POD metrics. The results of this study suggest further risks to the health of dwarf mountain pine and the ecological services they provide in the highly sensitive environment of the High Tatra Mountains.

Acknowledgements

This work was supported by the Slovak Research and Development Agency under contracts (No. APVV–0429–12, APVV–16–0325, APVV 0480-12), and by the Grant Agency of the Slovak Republic (VEGA, No. 2/0053/14, 2/0026/16, 1/0367/16). We also acknowledge the project ITMS 26220220066, funded by ERDF (10%). The authors are grateful to the Slovak Hydrometeorological Institute (SHMI) for providing meteorological, climatic, and EMEP data. The development of the DO_3SE model interface has been made possible through funding provided by the UK Department of Environment, Food, and Rural Affairs (DEFRA) and through institutional support provided to the Stockholm Environment Institute from the Swedish International Development Agency (SIDA).

Appendix A. Supplementary data

Supplementary data related to this article can be found at https://doi.org/10.1016/j.apr.2018.08.003.

References

Adame, J.A., Sole, J.G., 2013. Surface ozone variations at a rural area in the northeast of the Iberian Peninsula. Atmos. Pollut. Res. 4, 130–141. https://doi.org/10.5094/APR.2013.013.

Ashmore, M., Emberson, L., Karlsson, P.E., Pleijel, H., 2004. New Directions: a new generation of ozone critical levels for the protection of vegetation in Europe. Atmos. Environ. 38, 2213–2214. http://doi.org/10.1016/j.atmosenv.2004.02.029.

Bičárová, S., Sitková, Z., Pavlendová, H., 2016. Ozone phytotoxicity in the western Carpathian mountains in Slovakia. Lesn. Cas. For. J. 62, 77–88. https://doi.org/10.1515/forj-2016-0008.

Braun, S., Schindler, C., Rihm, B., 2014. Growth losses in Swiss forests caused by ozone: epidemiological data analysis of stem increment of Fagus sylvatica L. and Picea abies Karst. Environ. Pollut. 192, 129–138. http://doi.org/10.1016/j.envpol.2014.05.016.

Büker, P., Feng, Z., Uddling, J., Briolat, A., Alonso, R., Braun, S., Elvira, S., Gerosa, G., Karlsson, P.E., Le Thiec, D., Marzuoli, R., Mills, G., Oksanen, E., Wieser, G., Wilkinson, M., Emberson, L.D., 2015. New flux based dose-response relationships for ozone for European forest tree species. Environ. Pollut. 206, 163–174. https://doi.org/10.1016/j.envpol.2015.06.033.

Büker, P., Morrissey, T., Briolat, A., Falk, R., Simpson, D., Tuovinen, J.-P., Alonso, R., Barth, S., Baumgarten, M., Grulke, N., Karlsson, P.E., King, J., Lagergren, F., Matyssek, R., Nunn, A., Ogaya, R., Peñuelas, J., Rhea, L., Schaub, M., Uddling, J., Werner, W., Emberson, L.D., 2012. DO_3SE modelling of soil moisture to determine ozone flux to forest trees. Atmos. Chem. Phys. 12, 5537–5562. https://doi.org/10.5194/acp-12-5537-2012.

Bussotti, F., Desotgiu, R., Cascio, C., Pollastrini, M., Gravano, E., Gerosa, G., Marzuoli, R., Nali, C., Lorenzini, G., Salvatori, E., Manes, F., Schaub, M., Strasser, R.J., 2011. Ozone stress in woody plants assessed with chlorophyll a fluorescence. A critical reassessment of existing data. Environ. Exp. Bot. 73, 19–30. http://doi.org/10.1016/j.envexpbot.2010.10.022.

Bytnerowicz, A., Godzik, B., Grodzińska, K., Fraçzek, W., Musselman, R., Manning, W., Badea, O., Popescu, F., Fleischer, P., 2004. Ambient ozone in forests of the Central and Eastern European mountains. Environ. Pollut. 130, 5–16. http://doi.org/10.1016/j.envpol.2003.10.032.

Chevalier, A., Gheusi, F., Delmas, R., Ordóñez, C., Sarrat, C., Zbinden, R., Thouret, V., Athier, G., Cousin, J.-M., 2007. Influence of altitude on ozone levels and variability in the lower troposphere: a ground-based study for western Europe over the period 2001–2004. Atmos. Chem. Phys. 7, 4311–4326. https://doi.org/10.5194/acp-7-4311-2007.

CLRTAP, 2017. Mapping Critical Levels for Vegetation, Chapter III of Manual on methodologies and criteria for modelling and mapping critical loads and levels and air pollution effects, risks and trends. In: UNECE Convention on Long Range Transboundary Air Pollution, . https://www.icpmapping.org/Latest_update_Mapping_Manual.

Cooper, O.R., Parrish, D.D., Ziemke, J., Balashov, N.V., Cupeiro, M., Galbally, I.E., Zbinden, R.M., 2014. Global distribution and trends of tropospheric ozone: an observation-based review. Elem. Sci. Anth. 2, 29. http://doi.org/10.12952/journal.elementa.000029.

Coulston, J.W., Smith, G.C., Smith, W.D., 2003. Regional assessment of ozone sensitive tree species using bioindicator plants. Environ. Monit. Assess. 83, 113–127. http://doi.org/10.1023/A:1022578506736.

Dalstein, L., Vas, N., 2005. Ozone concentrations and ozone-induced symptoms on Coastal and alpine Mediterranean pines in southern France. Water, Air, Soil Pollut. 160, 181–195. http://doi.org/10.1007/s11270-005-4144-7.

De Marco, A., Sicard, P., Vitale, M., Carriero, G., Renou, C., Paoletti, E., 2015. Metrics of ozone risk assessment for Southern European forests: canopy moisture content as a potential plant response indicator. Atmos. Environ. 120, 182–190. http://doi.org/10.1016/j.atmosenv.2015.08.071.

Díaz-de-Quijano, M., Peñuelas, J., Ribas, À., 2009. Increasing interannual and altitudinal ozone mixing ratios in the Catalan Pyrenees. Atmos. Environ. 43, 6049–6057. http://doi.org/10.1016/j.atmosenv.2009.08.035.

Dizengremel, P., Jolivet, Y., Tuzet, A., Ranieri, A., Le Thiec, D., 2013. Integrative phytotoxic ozone dose assessment in leaves in view of risk modelling for forest ecosystems. In: In: Matyssek, R., Clarke, N., Cudlin, P., Mikkelsen, T.N., Tuovinen, J.-P., Wieser, G., Paoletti, E. (Eds.), Climate Change, Air Pollution and Global Challenges: Knowledge, Understanding and Perspectives from Forest Research, Elsevier Physical Sciences Series “Developments in Environmental Science”, vol. 13. pp. 267–283.

EEA, 2017. Report No 28/2017: Air Quality in Europe — 2017 Report. . http://www.eea.europa.eu/publications/air-quality-in-europe-2016.

Emberson, L.D., Ashmore, M.R., Cambridge, H.M., Simpson, D., Tuovinen, J.P., 2000. Modelling stomatal ozone flux across Europe. Environ. Pollut. 109, 403–413. http://doi.org/10.1016/S0269-7491(00)00043-9.

Emberson, L.D., Büker, P., Ashmore, M.R., 2007. Assessing the risk caused by ground level ozone to European forest trees: a case study in pine, beech and oak across different climate regions. Environ. Pollut. 147, 454–466. https://doi.org/10.1016/j.envpol.2006.10.026.

Feng, Z.Z., Büker, P., Pleijel, H., Emberson, L.D., Karlsson, P.E., Uddling, J., 2017. A unifying explanation for variation in ozone sensitivity among woody plants. Global Change Biol. 24, 1–7. https://doi.org/10.1111/gcb.13824promoting.

Fleischer, P., Pichler, V., Fleischer Jr., P., Holko, L., Máliš, F., Gömöryová, E., Cudlín, P., Holeksa, J., Michalová, Z., Homolová, Z., Skvarenina, J., Střelcová, K., Hlaváč, P., 2017. Forest ecosystem services affected by natural disturbances, climate and land-use changes in the Tatra Mountains. Clim. Res. 73/1, 1–15. https://doi.org/10.3354/cr01461.

Fuhrer, J., Skärby, L., Ashmore, M.R., 1997. Critical levels for ozone effects on vegetation in Europe. Environ. Pollut. 97, 91–106. http://doi.org/10.1016/S0269-7491(97)00067-5.

Gottardini, E., Cristofori, A., Cristofolini, F., Nali, C., Pellegrini, E., Bussotti, F., Ferretti, M., 2014. Chlorophyll-related indicators are linked to visible ozone symptoms: evidence from a field study on native Viburnum lantana L. plants in northern Italy. Ecol. Indicat. 39, 65–74. http://doi.org/10.1016/j.ecolind.2013.11.021.

Grünhage, L., Krause, G.H.M., Köllner, B., Bender, J., Weigel, H.J., Jäger, H.J., Guderian, R., 2001. A new flux-orientated concept to derive critical levels for ozone to protect vegetation. Environ. Pollut. 111, 355–362. http://doi.org/10.1016/S0269-7491(00)00181-0.

Hoshika, Y., Osada, Y., de Marco, A., Peñuelas, J., Paoletti, E., 2018. Global diurnal and nocturnal parameters of stomatal conductance in woody plants and major crops. Global Ecol. Biogeogr. 27, 257–275. https://doi.org/10.1111/geb.12681.

Hůnová, I., Novotný, R., Uhlířová, H., Vráblík, T., Horálek, J., Lomský, B., Šrámek, V., 2010. The impact of ambient ozone on mountain spruce forests in the Czech Republic as indicated by malondialdehyde. Environ. Pollut. 158, 2393–2401. http://doi.org/10.1016/j.envpol.2010.04.006.

ICP, 2017. ICP FORESTS 2016 Executive Report. . https://icp-forests.org/pdf/ER2016.pdf.

Karlsson, P.E., Braun, S., Broadmeadow, M., Elvira, S., Emberson, L., Gimeno, B.S., Le Thiec, D., Novak, K., Oksanen, E., Schaub, M., Uddling, J., Wilkinson, M., 2007. Risk assessments for forest trees: the performance of the ozone flux versus the AOT concepts. Environ. Pollut. 146, 608–616. http://doi.org/10.1016/j.envpol.2006.06.012.

Kasparoglu, S., Incecik, S., Topcu, S., 2018. Spatial and temporal variation of O3, NO and NO2 concentrations at rural and urban sites in Marmara Region of Turkey. Atmos. Pollut. Res. https://doi.org/10.1016/j.apr.2018.03.005.

Kefauver, S.C., Penuelas, J., Ribas, A., Díaz-de-Quijano, M., Ustin, S., 2014. Using Pinus uncinata to monitor tropospheric ozone in the Pyrenees. Ecol. Indicat. 36, 262–271. http://doi.org/10.1016/j.ecolind.2013.07.024.

Kopáček, J., Kaňa, J., Bičárová, S., Fernandez, I.J., Hejzlar, J., Kahounová, M., Norton, S.A., Stuchlík, E., 2017. Climate change increasing calcium and magnesium leaching from granitic Alpine catchments. Environ. Sci. Technol. 51/1, 159–166. https://doi.org/10.1021/acs.est.6b03575.

Lefohn, A.S., Malley, C.S., Simon, H., Wells, B., Xu, X., Zhang, L., Wang, T., 2017. Responses of human health and vegetation exposure metrics to changes in ozone concentration distributions in the European Union, United States, and China. Atmos. Environ. 152, 123–145. http://doi.org/10.1016/j.atmosenv.2016.12.025.

Massman, W.J., Musselman, R.C., Lefohn, A.S., 2000. A conceptual ozone dose-response model to develop a standard to protect vegetation. Atmos. Environ. 34, 745–759. http://doi.org/10.1016/S1352-2310(99)00395-7.

Massman, W.J., 1998. A review of the molecular diffusivities of H2O, CO2, CH4, CO, O3, SO2, NH3, N2O, NO, and NO2 in air, O2 and N2 near STP. Atmos. Environ. 32, 1111–1127. http://doi.org/10.1016/S1352-2310(97)00391-9.

Matyssek, R., Bytnerowicz, A., Karlsson, P.E., Paoletti, E., Sanz, M., Schaub, M., Wieser, G., 2007. Promoting the O3 flux concept for European forest trees. Environ. Pollut. 146, 587–607. http://doi.org/10.1016/j.envpol.2006.11.011.

Mezei, P., Jakuš, R., Pennerstorfer, J., Havašová, M., Škvarenina, J., Ferenčík, J., Slivinský, J., Bičárová, S., Bilčík, D., Blaženec, M., Netherer, S., 2017. Storms, temperature maxima and the Eurasian spruce bark beetle Ips typographus—an infernal trio in Norway spruce forests of the Central European High Tatra Mountains. Agric.

For. Meteorol. 242, 85–95. https://doi.org/10.1016/j.agrformet.2017.04.004.
Mills, G., Pleijel, H., Braun, S., Büker, P., Bermejo, V., Calvo, E., Danielsson, H., Emberson, L., Fernández, I.G., Grünhage, L., Harmens, H., Hayes, F., Karlsson, P.-E., Simpson, D., 2011. New stomatal flux-based critical levels for ozone effects on vegetation. Atmos. Environ. 45, 5064–5068. https://doi.org/10.1016/j.envpol.2015.09.038.
Musselman, R.C., Lefohn, A.S., Massman, W.J., Heath, R.L., 2006. A critical review and analysis of the use of exposure- and flux-based ozone indices for predicting vegetation effects. Atmos. Environ. 40, 1869–1888. http://doi.org/10.1016/j.atmosenv.2005.10.064.
Nebel, B., Matile, P., 1992. Longevity and senescence of needles in Pinus cembra. L. Trees 6, 156–161.
Nguyen, H.T., Kwon, E.E., Kim, K.-H., Pandey, S.K., Chambers, S., Kumar, P., Kang, C.H., Cho, S.-J., Oh, J.-M., Brown, R.J.C., 2017. Factors regulating the distribution of O3 and NOx at two mountainous sites in Seoul, Korea. Atmos. Pollut. Res. 8, 328–337. https://doi.org/10.1016/j.apr.2016.10.003.
Nunn, A.J., Wieser, G., Metzger, U., Löw, M., Wipfler, P., Häberle, K.-H., Matyssek, R., 2007. Exemplifying whole-plant ozone uptake in adult forest trees of contrasting species and site conditions. Environ. Pollut. 146, 629–639. http://doi.org/10.1016/j.envpol.2006.06.015.
Paoletti, E., Manning, W.J., 2007. Toward a biologically significant and usable standard for ozone that will also protect plants. Environ. Pollut. 150, 85–95. http://doi.org/10.1016/j.envpol.2007.06.037.
Sicard, P., De Marco, A., Dalstein-Richier, L., Tagliaferro, F., Renou, C., Paoletti, E., 2016. An epidemiological assessment of stomatal ozone flux-based critical levels for visible ozone injury in Southern European forests. Sci. Total Environ. 541, 729–741. http://doi.org/10.1016/j.scitotenv.2015.09.113.
Vollenweider, P., Günthardt-Goerg, M.S., 2006. Erratum to "Diagnosis of abiotic and biotic stress factors using the visible symptoms in foliage". Environ. Pollut. 137 (2005), 455–465. Environ. Pollut., 140, 562–571. http://doi.org/10.1016/j.envpol.2006.01.002.
Wagner, S., Kronberger, G., Beham, A., Kommenda, M., Scheibenpflug, A., Pitzer, E., Vonolfen, S., Kofler, M., Winkler, S., Dorfer, V., Affenzeller, M., 2014. Architecture and design of the heuristic lab optimization environment. In: In: Klempous, R., Nikodem, J., Jacak, W., Chaczko, Z. (Eds.), Advanced Methods and Applications in Computational Intelligence. Topics in Intelligent Engineering and Informatics, vol. 6. pp. 197–261. https://doi.org/10.1007/978-3-319-01436-4_10.
WHO, 2013. Review of Evidence on Health Aspects of Air Pollution - REVIHAAP Project: Final Technical Report. . http://www.euro.who.int/_data/assets/pdf_file/0004/193108/REVIHAAP-Final-technical-report.pdf.
Wieser, G., Manning, W.J., Tausz, M., Bytnerowicz, A., 2006. Evidence for potential impacts of ozone on Pinus cembra L. at mountain sites in Europe: an overview. Environ. Pollut. 139, 53–58. https://doi.org/10.1016/j.envpol.2005.04.037.
Zapletal, M., Pretel, J., Chroust, P., Cudlín, P., Edwards-Jonášová, M., Urban, O., Pokorný, R., Czerný, R., Hůnová, I., 2012. The influence of climate change on stomatal ozone flux to a mountain Norway spruce forest. Environ. Pollut. 169, 267–273. http://doi.org/10.1016/j.envpol.2012.05.008.
Zeppel, M., Logan, B.A., Lewis, J.D., Phillips, N., Tissue, D.T., 2013. In: Nocturnal Sap Flow and Stomatal Conductance: a Review, Conference paper.